Review of imaging-based measurement techniques for free surface flows involving sediment transport and morphological changes

Q1 Sandra Soares-Frazão

ABSTRACT

In order to validate the numerical methods aimed at the simulation of fast transient flows involving sediment transport and morphological changes, data are required. However, field data are scarce, or, if existing, are often inaccurate or incomplete, due to the difficulty to take reliable measurements in such difficult flow conditions. Laboratory experiments constitute a good alternative to obtain validation data for numerical models. When performing simplified experiments, a limited number of well-identified flow features can be highlighted if appropriate measurements are taken. Advances in experimental techniques in the last decades have significantly enlarged the field of possible data acquisition, especially thanks to the development of non-intrusive techniques such as digital imagery. Non-intrusive techniques are of paramount importance when considering sediment transport because a measurement device interacting with the flow would also modify the observed morphological features. In this paper, several imaging-based techniques are presented for water-level and bed evolution measurements. The key features and advantages are discussed but also the drawbacks of those techniques. The discussion is illustrated by different examples that have resulted in data sets commonly used by scientists all over the world to test their numerical simulation tools.

Key words | dam-break flow, experiments, imaging techniques, non-intrusive, sediment transport

Sandra Soares-Frazão
Institute of Mechanics, Materials and Civil Engineering,
Université catholique de Louvain,
Place du Levant 1, L5.05.01, 1348 Louvain-la-Neuve,
Belgium
E-mail: *sandra.soares-frazao@uclouvain.be*

HIGHLIGHTS

- Review of imaging-based measurement techniques to provide reliable data sets for the validation of numerical schemes.
- Application to water-level and bed evolution measurements.
- Application to velocity measurements, including surface-velocity and velocity field in the flow.
- Presentation of data sets with experimental data available to the scientific community.

INTRODUCTION

Significant progress has been achieved in the last decades regarding pure hydrodynamic flow modelling, with the developments of numerous commercial or open-source packages (e.g. Telemac, Mike, Flow2D, HEC, etc.). Coupled with GIS tools, these have allowed increasing the level of preparation of public authorities in charge of civil protection in flood-prone areas. Among other initiatives, the EU Flood directive has obliged all member states to provide the population with inundation and risk maps corresponding to different flood scenarios.

However, heavy floods might also result in strong erosion of riverbeds and soils. Such flows are observed all over the world at an increasing rate, due among others to climate change. Unfortunately, the development of flood

doi: 10.2166/hydro.2020.026

prediction tools involving sediment transport is not as developed as pure hydrodynamic tools. There is still no clear agreement in the scientific community regarding the best appropriate mathematical models and governing equations to predict morphological evolution. Moreover, the level of uncertainty regarding soil composition is often too important while reducing a riverbed to a single representative grain size can lead to strongly inaccurate results.

Unfortunately, it is very difficult to monitor morphodynamic flows *in situ*. Measuring the bed evolution of a real river during a flood event appears until now as an impossible task, in such a way that available data sets based on field measurements only provide scarce data about morphological evolution, obtained from a post-flood survey.

Laboratory experiments provide a means to partially circumvent this difficulty. Well-controlled and reproducible experiments can be performed, to prepare reliable data sets allowing for the validation of numerical simulation tools. However, there are two main difficulties regarding experiments with sediments. First, scaling issues have to be considered as the geometrical similitude (e.g. Froude similitude) that can be applied to pure hydrodynamic flows becomes hazardous with sediment. Indeed, depending on the full-scale sediment size, a simple geometrical reduction might result in a change of behaviour, from non-cohesive grains to very fine grains subject to cohesion effects. Therefore, a special care should be taken in the design of the experiments, in order to ensure that the appropriate features are properly measured. Instead of working with scale models, small-scale setups can be used, considered as prototypes having 1:1 scale, but still representative of features observed in nature. So, instead of using the measurements to scale up the results and interpret them at a larger scale, the results are interpreted directly, without any scaling. Such experiments are referred to as idealized experiments, as they are designed to highlight in a simplified way features that are observed in nature. An example is provided by the bank erosion experiments conducted by Soares-Frazão *et al.* (2007). In nature, as illustrated in Figure 1(a), bank erosion can result in a final quasi-trapezoidal shape of the valley, with planar banks. In the laboratory, as illustrated in Figure 1(b), an experiment of bank erosion was designed where the banks also present a planar shape after erosion because of the non-cohesive material used. So, despite the small size of the laboratory experiment compared to the real valley, the cross-section evolution is comparable to what can be observed in the field and the measurements can, thus, be used to validate numerical simulation tools used is real-flow situations.

A second issue regards the measurement techniques. Intrusive devices deployed into the flow might alter local sediment transport and completely change the morphological evolution. As an example, a level gauge or an ADV probe plunged into the water might induce unexpected local scouring. Therefore, non-intrusive techniques should preferably be used, especially when fast transient flows are considered, such as dam-break flows.

Digital imaging techniques offer a wide range of possibilities to obtain accurate measurements in flows involving sediment transport. Water levels can be measured if optical access to the flow is available through a glass wall (e.g. Soares-Frazão 2007; Juez *et al.* 2017). Alternatively, to

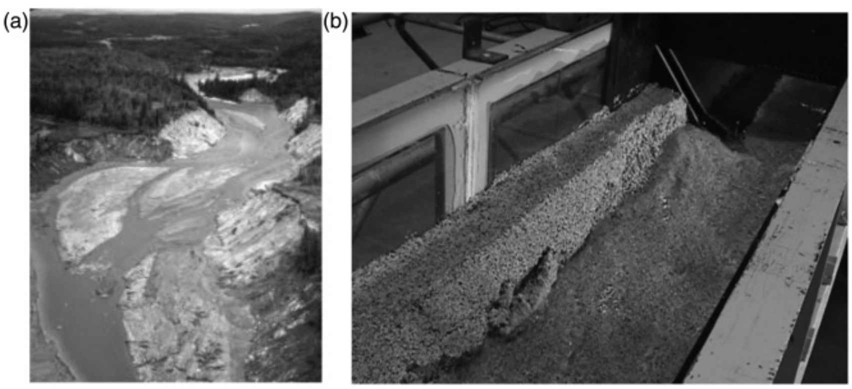

Figure 1 | Geomorphic consequences of dam-break flow. (a) Lake Ha!Ha! 1996 dam break (Brooks & Lawrence 1999) and (b) bank erosion experiment (Soares-Frazão *et al.* 2007).

obtain field data for the water level, an opaque texture has to be added to the water, as done, e.g., by Frank & Hager (2014) in their breaching experiments. This, however, can be used only for smooth water surfaces, and fast transient flows featuring sharp surface slopes or hydraulic jumps are excluded.

As regards the velocity field, two different situations can be considered: (i) the surface-velocity field and (ii) the velocity field in a vertical section of the flow. For surface velocities, using floating tracers or any easily identifiable feature on the free surface, velocity fields can be obtained using particle tracking velocimetry (PTV), as done, e.g., by Soares-Frazão & Zech (2007), or surface particle image velocimetry (PIV), as in Creëlle *et al.* (2018). For the vertical velocity distribution, flow illumination using a laser sheet allows to isolate one single cross-section to measure the velocity field during the flow using PTV or PIV techniques as done, e.g., by Aleixo *et al.* (2011) or Fent *et al.* (2019). Particle tracking was also successfully used by Persi *et al.* (2019) for floating wood debris in order to calibrate a dynamic Eulerian–Lagrangian model.

Finally, for the bed-level evolution, things become more complicated as it is necessary to have an optical access to the bed. Some recent developments using ultrasound imaging systems by Zou *et al.* (2018) allow to obtain three-dimensional reconstruction of the bathymetry in laboratory experiments. The process is, however, very complex and offers only a limited field of view. More classical imaging systems providing side views through glass walls allow to measure one-dimensional flows as done by Capart *et al.* (2002) for a dam-break flow, Juez *et al.* (2017) for a slope evolution experiment and Sadeghfam *et al.* (2019) for scouring. If a single section of the flow is to be observed, one can use a laser sheet as done by Fent *et al.* (2019) to isolate one particular flow section. However, depending on the bed morphology, it might be difficult to have an optical access to this section and it might be necessary to film the flow through the water surface (e.g. Soares-Frazão *et al.* 2007). In such cases, refraction effects have to account for.

Through a review of the recent literature about imaging techniques and based on the experience of the author, this paper aims at illustrating and discussing non-intrusive imaging techniques to obtain measurements in idealized dam-break flows involving intense sediment transport. The main techniques used in the selected experiments are first briefly presented. Then, based on experiments performed in the author's laboratory, a series of applications are illustrated, each corresponding to an idealized representation of flow features that can be observed in nature. For each application, a test case with available published data for the validation of numerical simulation tools is presented and the key challenges for numerical simulations are discussed.

DIGITAL IMAGERY FOR FREE SURFACE FLOW MEASUREMENTS

Water- and bed-level measurements

These measurements require an optical access to the flow. Different situations can be considered. The simplest case consists in placing a camera normal to the flume equipped with glass walls, assuming that the flow is constant over the width of the flume. If the camera is perpendicular to the flume and if it can be assumed that no distortion is induced by the lens, images as illustrated in Figure 2(a) can be obtained. The free surface can be easily identified and applying a detection procedure as described in Soares-Frazão (2007), the free surface can be extracted (Figure 2(b)).

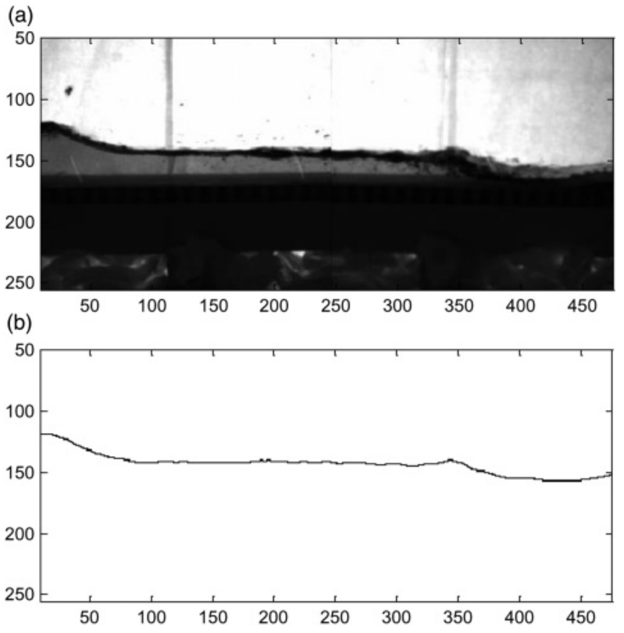

Figure 2 | Dam-break flow experiments over a triangular sill (Soares-Frazão 2007): (a) raw image and (b) detected free surface (axes in pixels).

The detection procedure consists in identifying at each abscissa in the image the vertical position of a sharp change in greyscale. This, of course, requires preparing the set-up in order to ensure a clear contrast at the flow free surface. The result is then transformed from image coordinates expressed in pixels to real-world coordinates based on a calibration of the images defined prior to the experiments.

If the assumption of constant velocity over the flume width is not valid, the technique can be improved by using a laser sheet to illuminate only a selected section of the flow. This was achieved by Fent *et al.* (2019) and is illustrated in Figure 3 for the case of a dam-break flow over a mobile bed. The detection procedure is based on the same principle as in the previous case: the rough image (Figure 3(a)) is treated using appropriate filters (Figure 3(b)) to enable the interface detection (Figure 3(c)).

If the camera cannot be placed perfectly perpendicular to the flow, it is still possible to use the interface detection methods but the transformation from image coordinates to real-world coordinates is more complex. Such a case is illustrated in Figure 4, where the camera is placed along the channel and makes an angle with the flow in order to 'see' a given cross-section of the flow illuminated by a laser sheet. The line to be detected is the trace of the laser on the channel bed. As can be observed in Figure 4(b), due to refraction by the water, this line is different above and below the water surface. The treatment and especially the procedure to transform the detected line into real-world coordinates is, thus, still more complex, based on affine transformations to account for the angle of view of the camera and the fact that the detected line is above or below the free surface as described in Soares-Frazão *et al.* (2007).

Velocity measurements

Velocity measurements using digital imaging techniques are based on particle tracking in the flow. Two main methods can be used: the PTV that can be used when the single

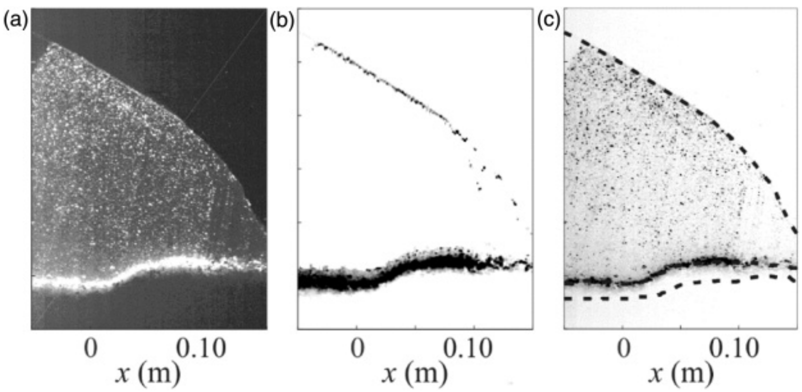

Figure 3 | Dam-break flow experiments over a mobile bed. Water and bed elevation detection from a laser-illuminated section of the flow.

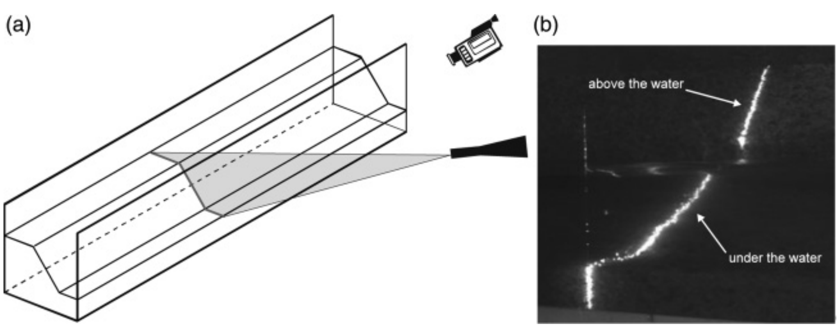

Figure 4 | (a) Laser-sheet measurement technique and (b) image obtained before treatment (Soares-Frazão *et al.* 2007).

particles can be followed from one image to the other, and the PIV that is based on correlation peaks for the position of particles in portions of the image, referred to as interrogation windows.

The PTV technique was already described by Malik *et al.* (1993) and then developed by Capart *et al.* (2002) and Spinewine *et al.* (2003) for idealized dam-break flow over sediment bed, where the sediments were represented by plastic particles of a few millimetres diameter. As described by Capart *et al.* (2002) and illustrated in Figure 5, the key steps of the method to treat a series of images recorded at a known frequency are (i) identifying the tracer particles on each image (Figure 5(a)); (ii) finding corresponding particles on the successive images using a Voronoi-based tracking methodology (Figure 5(b)) and (iii) calculating the distance travelled by each particle to obtain the local velocity (Figure 5(c)). The key issue to apply this PTV method is that the minimum size of the particles on the filmed images should be about 4–6 pixels to allow accurate detection. However, with the high resolution of even common cameras nowadays, this is, in general, not a problem.

This methodology was also successfully applied to obtain surface-velocity fields in fast transient flows seeded with floating particles as described in Soares-Frazão & Zech (2007). Using neutrally buoyant particles (high-density polyethylene with a mean diameter of 2 mm), the technique was applied to the measurement of the vertical velocity field in a dam-break flow over a fixed bed by Aleixo *et al.* (2011), as illustrated in Figure 6.

PIV has become in the last years an established technique (Keane & Adrian 1992; Raffel *et al.* 2007; Tropea *et al.* 2007) to measure velocity fields from filmed images in flows seeded with small tracer particles. The major difference

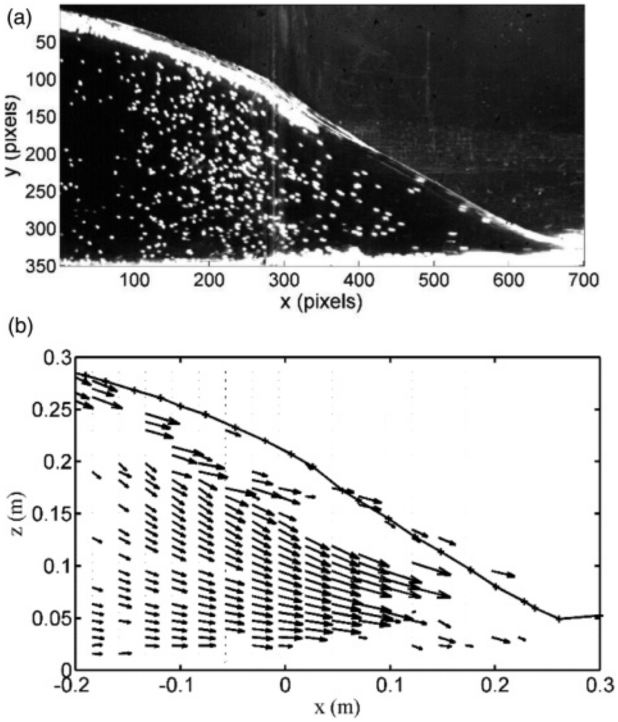

Figure 6 | PTV applied to a dam-break flow over fixed bed (Aleixo *et al.* 2011): (a) rough image in pixel coordinates with the neutrally buoyant particles and (b) resulting velocity field in real-world coordinates.

between the PIV and the PTV is on the working principle: PTV tracks individual particles, while PIV uses the patterns of particles to determine by correlation their most probable displacement between two successive images recorded with a very small time interval (Raffel *et al.* 2007). Both images are then divided into smaller areas, called interrogations windows. By correlating the correspondent interrogation windows at time t and time $t + dt$, the displacement of the correlation peak ds of the considered interrogation window is found and the most probable velocity can be calculated.

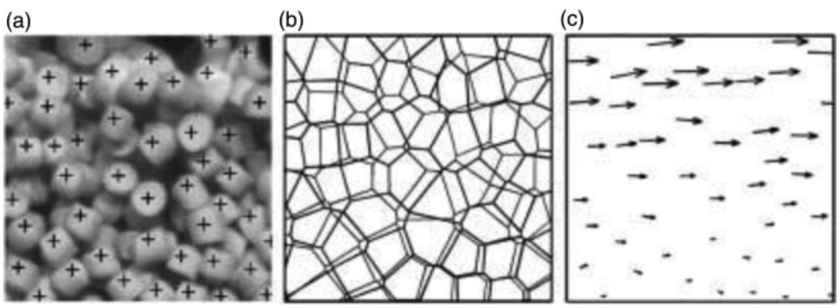

Figure 5 | PTV following Capart *et al.* (2002): (a) particle detection, (b) matching of Voronoi diagram around the particles from two successive images and (c) resulting velocity field.

This technique was applied by Fent *et al.* (2019) to measure the velocity field in the dam-break flow over a mobile bed illustrated in Figure 2. Here, the particles used were pliolite particles of about 0.5 mm mean diameter, much smaller than the particles used by Aleixo *et al.* (2011). As can be observed, the flow is seeded with small pliolite particles that are illuminated by the laser sheet. Applying PIV yields the results illustrated in Figure 7.

In these examples, PIV was applied to a vertical section of the flow. However, the technique can also be used to measure the velocity at the free surface of the flow (e.g. Creelle *et al.* 2018). This type of application is referred to as 'Large-scale PIV' as described already by Fujita *et al.* (1998). In these cases, the PIV methodology is applied to floating tracers for laboratory experiments. The technique can be applied in the field, by tracking floating tracers or even irregularities of the free surface, like small waves, assuming that these irregularities travel at the same speed as water and that they can be detected and followed by the LSPIV algorithm. This LSPIV technique is becoming more and more popular for flow measurements in natural rivers, but will not be further discussed here.

Common features and requirements of imaging techniques

All image-based measurement techniques present some common features. First, a good optical access to the flow is needed, as well as an appropriate calibration procedure to translate the image measurements from pixel coordinates to real-world coordinates. This procedure is simple when the images are taken normal to the measurement plane. However, when the camera position is such that it makes an angle with the measurement plane, appropriate affine transformations should be used. If the bed evolution is measured, refraction effects through the water surface should be accounted for.

Then, the considered experiment should be highly reproducible. Indeed, in order to obtain a complete set of data covering a wide spatial and temporal range of the phenomenon, the experiment has to be repeated several times. This reproducibility ensures that the measurements obtained for different runs of the same experiment can be combined into a single data set.

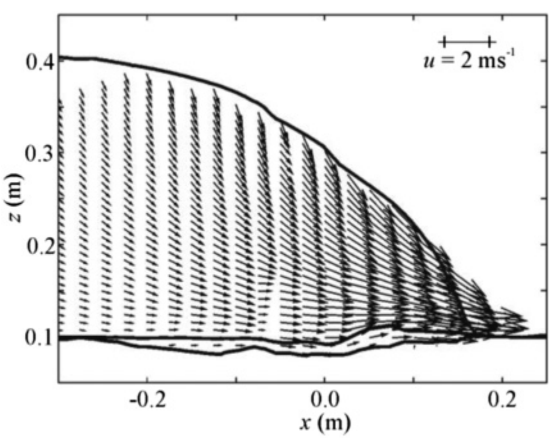

Q8 **Figure 7** | PIV measurements applied to a dam-break flow over mobile bed (Fent *et al.* 2019).

APPLICATIONS

Several applications are presented in the next sections, for which experimental data are available to validate numerical models. All the experiments presented here were conducted at the Hydraulics Laboratory of the Institute of Mechanics, Materials and Civil Engineering at UCLouvain, Belgium.

Transient flows over steep sloping beds

In steep catchments and mountainous rivers, erodible bed channels are modified through sediment transport, which takes place as bedload. Sediment supply can be increased by soil erosion caused by heavy rainfall or decreased after the installation of sediment trapping systems. The sediment transport capacity of a stream can also be altered during floods when the water discharge significantly increases. One type of visible evolution is the migration of a local change in the bed slope, referred to as a knickpoint. Several knickpoint configurations exist in nature and the morphological evolution is governed by the bedload capacity and hydraulic conditions.

This situation can be represented in the laboratory as an initial knickpoint separating an upstream mild slope from a downstream steep slope, the knickpoint being progressively eroded by the flow. A first idealized representation of such a flow in a knickpoint configuration was studied by Bellal *et al.* (2004) and Bellal *et al.* (2009), however, for small slopes differences between the upstream and downstream bed slope.

In the study of Juez *et al.* (2017), an extreme situation compared to the previous configurations was considered, as shown in Figure 8. The initial bed slopes in the upstream and downstream parts were 5.05 and 17.6%, respectively. This experiment was carried out with an initial zero water discharge that was progressively increased to 0.001 m^3/s in 10 s. The wetting front progressively migrated towards the knickpoint and started eroding it. From that moment, the evolution was fast and the downstream steep slope was softened to an equilibrium value of 7.8% all over the flume. Since the peak erosion took place in just a few seconds, only non-intrusive imaging techniques allow to follow and decompose this very fast bed evolution. An example is illustrated in Figure 9.

From the numerical modelling point of view, these tests aim at assessing the capability of numerical simulation tools to reproduce the bed morphological evolution in time over steep bed slopes. The key challenge concerns the applicability of classical sediment transport formula and bed shear stress calculation to steep bed slopes where the difference between the water elevation above the bed $z_w - z_b$ measured along the z-coordinate and the water depth h measured normal to the bed becomes non-negligible.

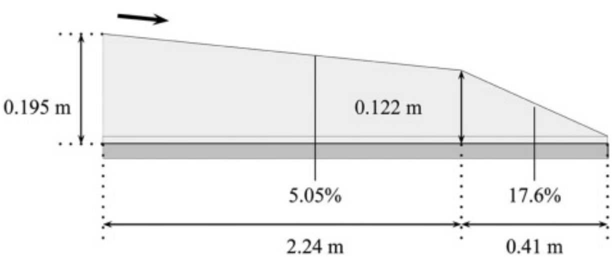

Figure 8 | Experimental set-up for the knickpoint test (Juez *et al.* 2017).

From the experimental point of view, the key challenge consists of measuring simultaneously the water and bed surface through the glass walls of the channel. Thanks to laser-sheet illumination, these surfaces appear as a white line on the recorded images. Using appropriate image correction and calibration procedures, these surfaces can be transformed into water surface and bed profiles in a global reference system.

One-dimensional dike overtopping

One of the most important dike failure mechanisms is by overtopping. Such an overtopping, caused by the failure of the spillway gates opening system, resulted in the complete failure of the Tous dam in 1982 as reported by Alcrudo & Mulet (2007). A similar catastrophe could be avoided for the Oroville dam in 2017 (Koskinas *et al.* 2019; Vano *et al.* 2019): due to discharge above the capacity of the service spillway, the emergency spillways were used, resulting in strong erosion of the unprotected downstream face of this earthen embankment but fortunately, the complete failure could be avoided. According to Visser (1995), several stages can be observed during a dike failure, with in particular the progressive erosion of the dike crest, the transport of the eroded material further downstream and the progressive flattening of the downstream face slope that is initially steep from a hydraulic point of view. Q2

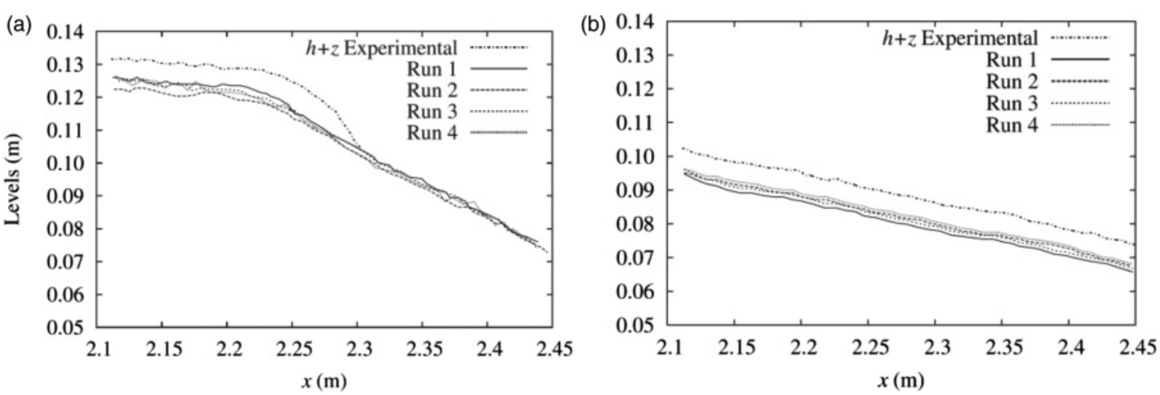

Figure 9 | Evolution of the bed- and water-level profiles at time (a) 16.05 s and (b) 80.80 s (Juez *et al.* 2017). Q9

Such a dike overtopping was reproduced in the laboratory in a simplified one-dimensional version by Van Emelen *et al.* (2015). This one-dimensional embankment overtopping is representative for the overtopping of a slice of a wide embankment. As shown in Figure 10, an initial sand dike was built in a 10-m long and 0.2-m wide high horizontal flume. The embankment height is 0.20 m, the crest length 0.10 m and the upstream and downstream slopes are 1 V:2 H. A 0.05-m thick layer of sand is placed downstream of the embankment, over a length of 1 m. This additional sand layer allows studying the possible bed erosion downstream of the embankment, due to the flood generated by the dike break, and also acts as a natural drain for the embankment, avoiding any premature sliding of the downstream slope due to seepage through the embankment.

The sand has a uniform size distribution with $d_{50} =$ 0.61 mm and the Manning friction coefficient was estimated as $0.015\,\mathrm{sm}^{-1/3}$. To ensure a good compaction of the embankment, and the repeatability of the tests, a precise procedure is followed to build and compact it. A 2-m long and 1.2-m wide storage reservoir is located upstream of the embankment, with an initial water level of 0.17 m. The inflow in the reservoir is progressively increased at a constant rate of $0.25\,\mathrm{s}^{-2}$ until reaching a constant value of $2.5\,\mathrm{s}^{-1}$, which is maintained during all the overtopping test duration. Downstream of the flume, water and sand flow freely into a lower reservoir. The progressive evolution of the embankment is illustrated in Figure 11.

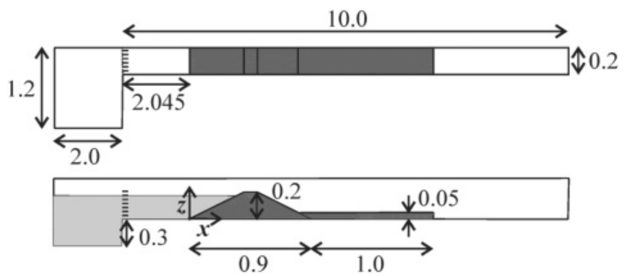

Figure 10 | Flume and embankment geometry (in metres): plane view (above) and elevation (below) (from Van Emelen *et al.* (2015)).

From the numerical modelling point of view, the key challenge in this test is the computation of the correct sediment transport rate as the water flows over a very steep slope, far steeper than the range of validity of classical sediment transport formulations. As detailed in Van Emelen *et al.* (2015), sediment transport in this test case occurs as sheet flow, as the actual bed shear stress is far above the critical shear stress. It thus allows testing different bedload and sheet flow sediment transport formulations, as well as slope correction factors to account for the reduced bed stability over steep slopes.

Two-dimensional dam-break flow over a mobile bed

Following a dam or dike failure, the water flows not only in the initial riverbed but also inundates large areas located behind the dike. For embankments built along rivers, a

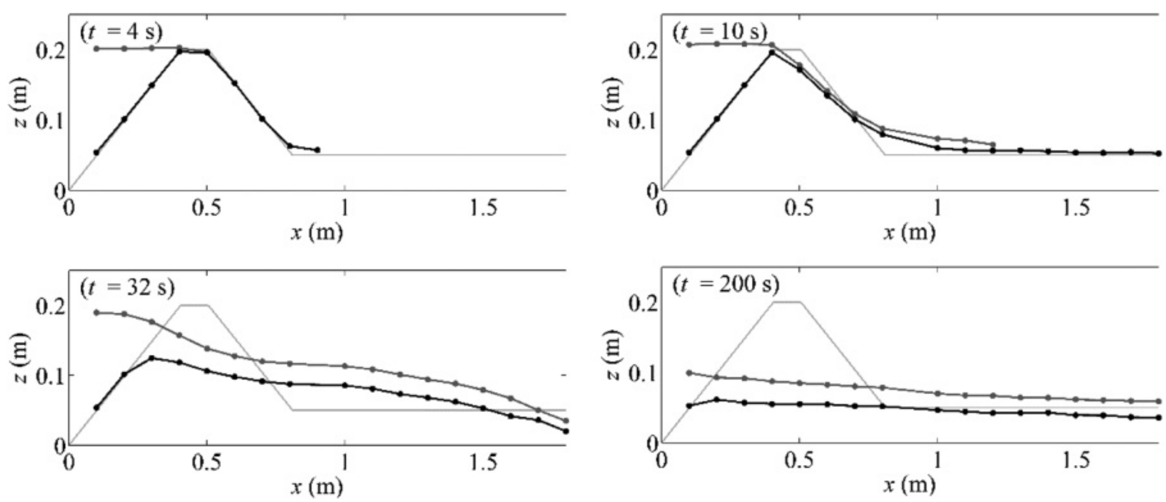

Figure 11 | Embankment (black curve) and water (grey curve) profiles at different times – initial dike in light grey (from Van Emelen *et al.* (2015)). Q10

local failure results in a flow invading an area that is usually not subject to flooding because it is expected to be protected by the dike. Such a situation was reproduced by Soares-Frazão *et al.* (2012), where a dam-breaching flow inundates a wide downstream floodplain, resulting in strong scouring immediately downstream of the breach and deposition around the scour hole. As described by the authors, this test case has been used as a benchmark for assessing the capabilities of numerical simulation tools and the efficiency of different modelling options.

The experimental set-up is illustrated in Figure 12. The experiment consists in reproducing a dam-break flow in a 3.6-m wide channel with an initial 0.085-m thick sediment layer. Two different configurations were considered: a dry-bed case, where the sediments in the downstream part were just saturated with water, and a wet-bed case with a layer of 0.065 m water above the downstream sediment layer. The upstream reservoir was filled with 0.47 m of water in the dry-bed case, and the water was suddenly released by the opening of a 1-m wide gate in the dam. The resulting flow rapidly spread over the entire channel, with intense bed erosion close to the failed dam and sediment deposition further downstream. The bed material consisted of uniform sand with a Manning friction coefficient of 0.0165 $m^{-1/3}$ s, the friction coefficient of the fixed bed being 0.010 $m^{-1/3}$ s. At the downstream end of the flume, a sediment trapping system stops their progression, and the water was collected in a tank. As explained in Soares-Frazão *et al.* (2012), this device had no influence over the duration of the test. After 20 s, no more bed evolution was observed so that the gate could be closed and the channel slowly emptied. The final bed topography was then measured using a laser technique, yielding a detailed final DTM as illustrated in Figure 13 for the dry-bed case. Q3 From these DTMs, measured with a horizontal resolution of 0.05 m, longitudinal or transversal profiles can be extracted.

No bed evolution could be measured during the flow, due to a poor optical access to the bed that is even worsened by the very irregular water surface and the presence of

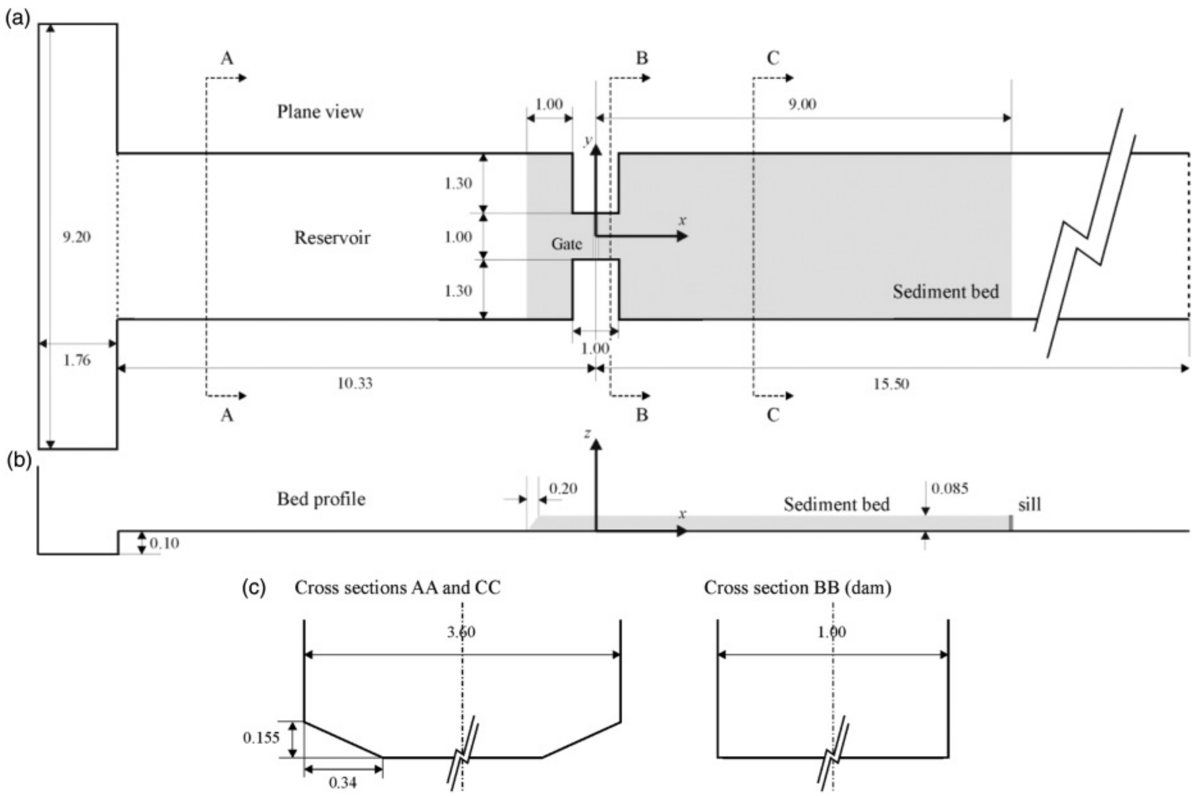

Figure 12 | Flume dimensions (in metres): (a) plane view, (b) elevation and (c) cross-sections.

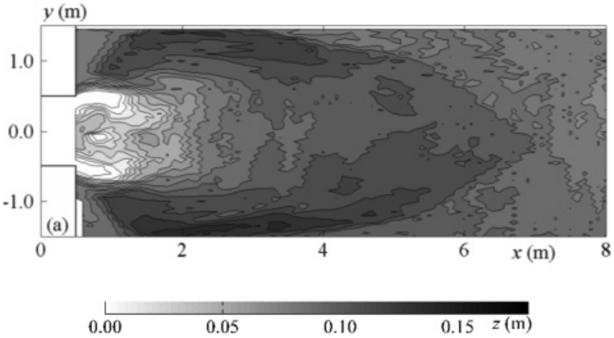

Q11 **Figure 13** | Final bed topography for the dry-bed case (from Soares-Frazão *et al.* (2012)).

hydraulic jumps. However, water-level measurements could be obtained during the flow at several locations. As illustrated in Soares-Frazão *et al.* (2012), a good reproducibility of the experiments could be achieved, despite the large dimensions of the flume, thanks to a fixed procedure followed to prepare the experiments and compact the initial bed layer in a reproducible way.

From the numerical point of view, the key challenge in this test case is the correct prediction of the scouring depth downstream of the failed dam, as well as the deposition height around the scour hole (Figure 12). It was shown in Soares-Frazão *et al.* (2012) that the simulation results were highly dependent on the mesh size and on the closure equations selected to predict sediment transport.

Dam-break flow in a channel with erodible banks

In case of very strong flows in natural rivers, the banks can be eroded and the valley completely reshaped. Such a case is illustrated in Figure 1 for the lake Ha! Ha! dike break reported by Brooks & Lawrence (1999) and Capart *et al.* (2007). In particular, it can be observed that the eroded banks present a slope equal to the natural angle of repose of the bank material. Such a situation is represented in Soares-Frazão *et al.* (2007), where the morphological evolution of a channel made of uniform sand with an initial trapezoidal shape is investigated. As illustrated in Figure 14, the set-up consists of a half cross-section with initial steep banks. Assuming a symmetrical behaviour of the flow, this choice of half cross-section allows an optical access to flow. The bed and bank material consist of uniform grains with $d_{50} = 1.8$ mm.

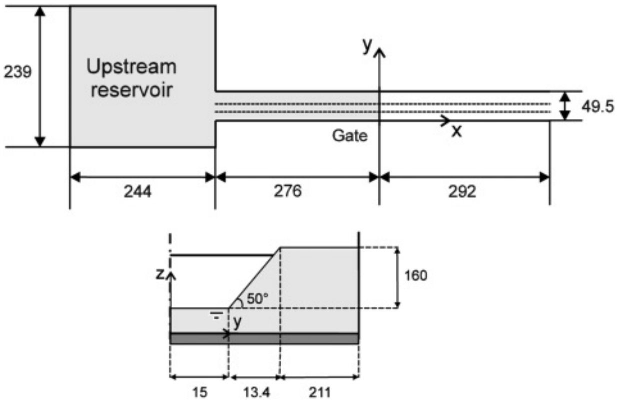

Figure 14 | Experimental set-up: (a) plane view and (b) cross-section. All dimensions in centimetres.

By rapidly lifting up the gate separating the reservoir from the channel, a dam-break flow is created that strongly reshapes the cross-section. Thanks to the optical access through the glass walls of the flume, the laser-sheet technique could be used to monitor the time evolution of the entire cross-section. Again, a key challenge to obtain valuable data is to achieve a good reproducibility of the experiments. Therefore, a fixed procedure to build the initial trapezoidal shape ensuring the same level of compaction between runs was followed.

The channel evolution after 4.9 s after gate opening is shown in Figure 15. Despite the fact that bank erosion appears as a random process with entire blocks falling into the water, a good reproducibility of the experiments was observed.

Sample results at cross-sections S1 and S6, located, respectively, 0.25 and 1.50 m downstream from the gate

Figure 15 | Trapezoidal channel evolution at $t = 4.9$ s (from Soares-Frazão *et al.* (2007)).

(located at $x = 0$ m) are illustrated in Figure 16. It can be observed that the initial steep bank slope is progressively smoothened by the flow, the final bank angle being equal to the angle of stability of the bed material.

From the numerical modelling point of view, this test case is challenging as it requires simulating bank erosion processes with an appropriate mathematical formulation. Indeed, if only bed erosion is considered, then the banks might become unrealistically steep. However, the mathematical formulation to describe this bank collapse process is not straightforward, as well as the coupling with the flow model.
Q4 Swartenbroekx *et al.* (2010) or Franzini & Soares-Frazão (2018) developed a geometric procedure where the local bank angle is compared to the angle of stability of the bed material and adapted to simulate the mass failure of the bank. The key challenge when implementing such procedures is to guarantee mass conservation of water and sediment while accounting for the possible instability of neighbouring portions of the bank after a local failure event.

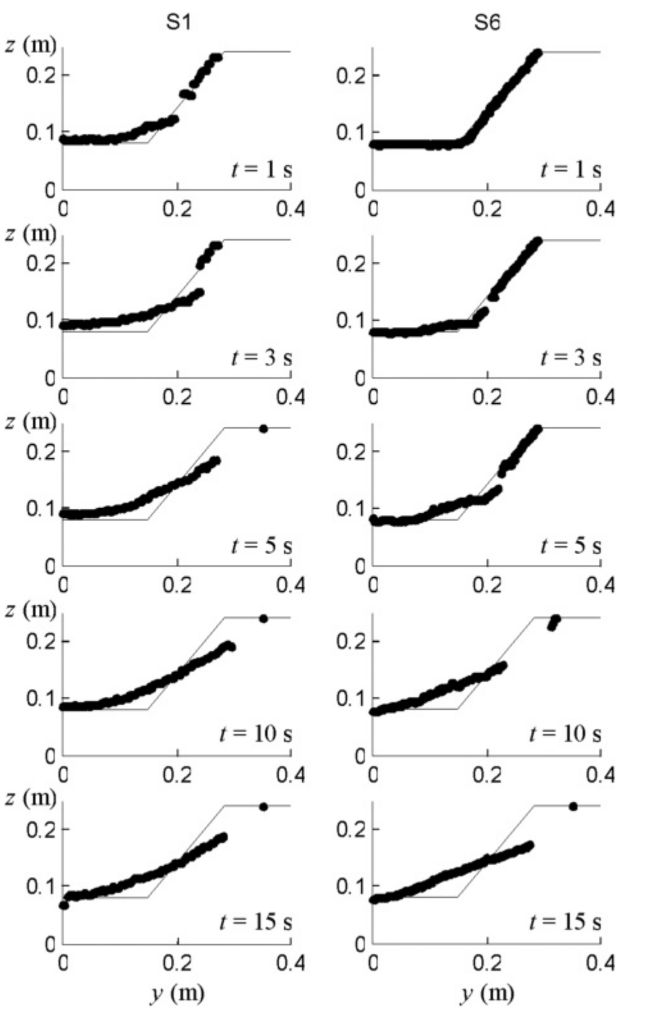

Figure 16 | Evolution of sections S1 ($x = 0.25$ m, left column) and S6 ($x = 1.50$ m, right column) at times $t = 1$ s, $t = 3$ s, $t = 5$ s, $t = 10$ s and $t = 15$ s (from Soares-Frazão *et al.* (2007)).

One-dimensional dam-break flow over a mobile bed

A key difficulty with numerical simulations of flows involving morphological changes by erosion and deposition is the choice of the sediment transport equations, as highlighted, e.g., by Van Emelen *et al.* (2015). Besides the choice of the sediment transport equation, a key issue is the calculation of the bed shear stress that appears in all these formulations. This bed shear stress depends on the energy slope that is usually expressed using Manning-type equations, originally developed for uniform-flow conditions. However, in severe transient conditions, when the flow is not yet fully developed, the bed shear stress might be significantly different. In order to investigate the velocity distribution close to the bed where sediments are entrained, a dam-break flow experiment allowing for the measurement of the velocity field was designed, still using non-intrusive imaging techniques. This test also allows for investigating the bed evolution in an idealized one-dimensional configuration, as proposed by Spinewine & Zech (2007) who studied dam-break flows over different bed materials and measuring only the bed and water levels. Then, taking advantage of the PIV technique, Fent *et al.* (2019) could measure the velocity distribution in the flow.

The set-up used by Fent *et al.* (2019) is illustrated in Figure 17, the flume being 0.25 m wide and equipped with glass walls for optimal optical access and a downward

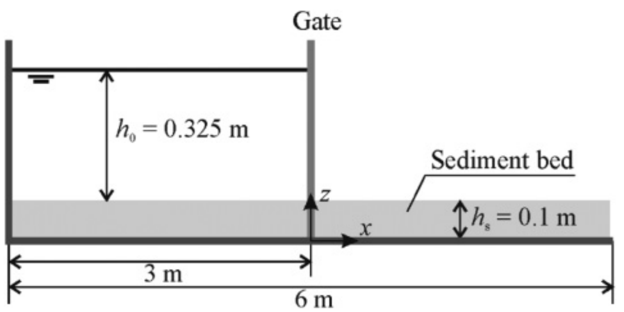

Figure 17 | Experimental set-up. Q12

moving gate to prevent sediment from being entrained in the flow by the gate movement. The sediment bed consists of uniform grains with a median diameter $d_{50} = 1.72$ mm. Measurements were taken through the glass walls of the flume using a fast camera at a rate of 500 images per second. In order to apply the PIV technique for the water layer, the reservoir was seeded with neutrally buoyant pliolite particles that appear as with points on the images. A laser sheet allowed to illuminate a longitudinal section of the flow as illustrated in Figure 3.

Applying the PIV analysis to the clear water layer and the moving sediment allowed to obtain a velocity field over the whole image. A limit detection procedure was also applied to identify the water surface, the limit between the fixed and mobile bed, and the limit between moving sediment and clear water (Figure 6). These limits could be identified thanks to brightness thresholds as no suspension occurs in the present case.

Example results for the horizontal velocity profiles in both the sediment and water layers are shown in Figure 18,

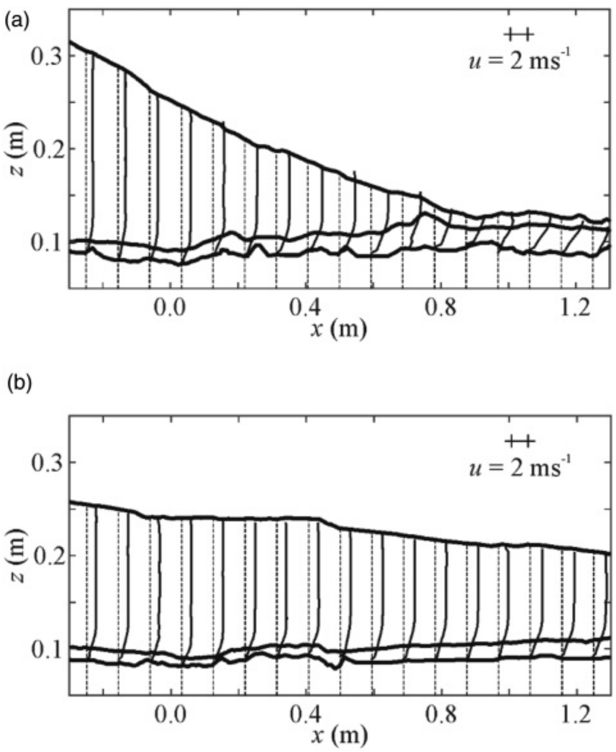

Q13 **Figure 18** | Distribution of the horizontal velocity component in the moving sediment and water layer at (a) $t = 0.7$ s and (b) $t = 2.0$ s (Fent *et al.* 2019).

where the thick lines indicate the limits between layers. The detailed measurements available for this case allow for the validation of both depth-averaged numerical models aiming at predicting the bed evolution following a one-dimensional dam-break flow, but also 2D-V models able to reproduce the velocity field over the depth. Moreover, the measurements can also be used to analyse different features in the flow such as the velocity profile and the related bed shear stress, or the pressure distribution in the flow.

CONCLUSIONS

In order to take measurements in fast free surface flows involving sediment transport, non-intrusive measurement techniques are recommended as they do not perturb the flow and, thus, do not induce parasitic sediment movement such as local scouring. Digital imagery, discussed in this paper, is such a technique allowing to record data over a whole field of the flow: a free surface profile, a bed elevation profile or a velocity field. However, imagery techniques require an optical access to the flow, either through the sidewalls of the flume or through the water surface. In this case, special care has to be taken to account for possible refraction effects.

The use of a laser sheet allows taking measurements in a spatially well-defined area by enlightening a selected cross-section of the flow. When any type of particles is available in the water column that can be illuminated by the laser sheet, particle tracking methods can be applied to measure velocities.

A key element for using such techniques is to properly design the experiment. First, it should be easily performed in the lab and be reproducible in order to allow for combining several runs to form a complete data set. When sediments are concerned, an appropriate methodology to prepare the experiment should be designed to ensure the reproducibility of the experiments. Indeed, different levels of compaction or initial sand moisture can result in different results regarding water levels and velocities. Secondly, a good optical access to the flow and uniform light conditions should be achieved. Uniform light conditions ensure a uniform treatment of the images where key features of the flow can be easily identified in order to allow for automated treatment. Finally, a reference system should be defined and a proper calibration is performed together with the measurements to allow for the transformation from image coordinates in pixels to real-world coordinates. The calibration procedure should consider possible refraction effects that might depend on the water depth.

In this paper, we have presented several test cases that were designed according to these guidelines and that form data sets usable for the validation of numerical models. Each data set highlights particular features of the flow in an idealized way that is, however, representative of some aspects of real-flow features that can be observed in the field.

ACKNOWLEDGEMENTS

The author acknowledges all his past and current researchers and collaborators who have contributed to the production of the data sets presented here.

DATA AVAILABILITY STATEMENT

All relevant data are included in the paper or its Supplementary Information.

REFERENCES

Alcrudo, F. & Mulet, J. 2007 Description of the Tous Dam break case study (Spain). *Journal of Hydraulic Research* **45** (Extra Issue), 45–57.

Aleixo, R., Soares-Frazão, S. & Zech, Y. 2011 Velocity-field measurements in a dam-break flow using a PTV Voronoï imaging technique. *Experiments in Fluids* **50**, 1633–1649.

Bellal, M., Iervolino, M. & Zech, Y. 2004 Knickpoint migration process: experimental and numerical approaches. In: *Proceedings 12th Conference on Sediment and Sedimentation Particles*, September 2004, Prague, Czech Republic, pp. 185–195.

Bellal, M., Capart, H., Soares-Frazão, S. & Zech, Y. 2009 Analytical, experimental, and numerical models of knickpoint migration. In: *Proceedings of the 7th IAHR Symposium on River, Coastal and Estuarine Morphodynamics*, Santa Fe Argentina, pp. 57–63.

Brooks, G. R. & Lawrence, D. E. 1999 The drainage of the Lake Ha! Ha! Reservoir and downstream geomorphic impacts along Ha! Ha! River, Saguenay Area, Quebec, Canada. *Geomorphology* **28**, 141–168.

Capart, H., Young, D. L. & Zech, Y. 2002 Voronoï imaging methods for the measurement of granular flow. *Experiments in Fluids* **32**, 121–135.

Capart, H., Spinewine, B., Young, D. L., Zech, Y., Brooks, G. R., Leclerc, M. & Secretan, Y. 2007 The 1996 Lake Ha! Ha! breakout flood, Québec: test data for geomorphic flood routing methods. *Journal of Hydraulic Research* **45** (Extra Issue), 97–109.

Creëlle, S., Roldan, R., Herremans, A., Meire, D., Buis, K., Meire, P., Van Oyen, T., De Mulder, T. & Troch, P. 2018 Validation of large-scale particle image velocimetry to acquire free-surface flow fields in vegetated rivers. *Journal of Applied Water Engineering and Research* **6** (3), 171–182.

Fent, I., Zech, Y. & Soares-Frazão, S. 2019 Dam-break flow experiments over mobile bed: velocity profile. *Journal of Hydraulic Research* **57** (1), 131–138.

Frank, P. J. & Hager, W. H. 2014 Spatial dike breach: accuracy of photogrammetric measurement system. In: *Proceedings of the International Conference on Fluvial Hydraulics, River Flow 2014*, pp. 1647–1654. Q5

Franzini, F. & Soares-Frazao, S. 2018 Coupled finite-volume scheme with adapted Augmented Roe scheme for simulating morphological evolution in arbitrary cross-sections. *Journal of Hydroinformatics* **20** (5), 1111–1130.

Fujita, I., Muste, M. & Kruger, A. 1998 Large-scale particle image velocimetry for flow analysis in hydraulic engineering applications. *Journal of Hydraulic Research* **36** (3), 397–414.

Juez, C., Soares-Frazão, S., Murillo, J. & Garcia-Navarro, P. 2017 Experimental and numerical simulation of bed load transport over steep slopes. *Journal of Hydraulic Research* **55** (4), 455–469.

Keane, R. & Adrian, R. 1992 Theory of cross-correlation analysis of PIV images. *Applied Science Research* **49**, 191–215.

Koskinas, A., Tegos, A., Tsira, P., Dimitriadis, P., Iliopoulou, T., Papanicolaou, P., Koutsoyiannis, D. & Williamson, T. 2019 Insights into the Oroville dam 2017 Spillway incident. *Geosciences* **9** (1), 37.

Malik, N. A., Dracos, T. H. & Papantoniou, D. A. 1993 Particle tracking velocimetry in three-dimensional flows – part II: particle tracking. *Experiments in Fluids* **15** (4–5), 279–294.

Persi, E., Petaccia, G., Sibilla, S., Brufau, P. & García-Navarro, P. 2019 Calibration of a dynamic Eulerian-Lagrangian model for the computation of wood cylinders transport in shallow-water flow. *Journal of Hydroinformatics* **21** (1), 164–179.

Raffel, M., Willert, C., Werely, S. & Kompenhans, J. 2007 *Particle Image Velocimetry – A Practical Guide*. Springer-Verlag. Q6

Sadeghfam, S., Daneshfaraz, R., Khatibi, R. & Minaei, O. 2019 Experimental studies on scour of supercritical flow jets in upstream of screens and modelling scouring dimensions using artificial intelligence to combine multiple models (AIMM). *Journal of Hydroinformatics* **21** (5), 893–907.

Soares-Frazão, S. 2007 Experiments of dam-break wave over a triangular bottom sill. *Journal of Hydraulic Research* **45** (Extra Issue), 19–26.

Soares-Frazão, S. & Zech, Y. 2007 Experimental study of dam-break flow against an isolated obstacle. *Journal of Hydraulic Research* **45** (Extra Issue), 27–36.

Soares-Frazão, S., Le Grelle, N., Spinewine, B. & Zech, Y. 2007 Dam-break induced morphological changes in a channel with uniform sediments: measurements by a laser-sheet imaging technique. *Journal of Hydraulic Research* **45** (Extra Issue), 87–95.

Soares-Frazão, S., Canelas, R., Cao, Z., Cea, L., Chaudhry, H. M., Die Moran, A., El Kadi, K., Ferreira, R., Cadórniga, I. F., Gonzalez-Ramirez, N., Greco, M., Huang, W., Imran, J., Le Coz, J., Marsooli, R., Paquier, A., Pender, G., Pontillo, M., Puertas, J., Spinewine, B., Swartenbroekx, C., Tsubaki, R., Villaret, C., Wu, W., Yue, Z. & Zech, Y. 2012 Dam-break flows over mobile beds: experiments and benchmark tests for numerical models. *Journal of Hydraulic Research* **50** (4), 364–375.

Spinewine, B. & Zech, Y. 2007 Small-scale laboratory dam-break waves on movable beds. *Journal of Hydraulic Research* **45** (Extra Issue), 73–86.

Spinewine, H., Capart, H., Larcher, M. & Zech, Y. 2003 Three-dimensional Voronoï imaging methods for the measurement of near-wall particulate flow. *Experiments in Fluids* **34**, 227–241.

Swartenbroekx, C., Soares-Frazão, S., Staquet, R. & Zech, Y. 2010 Two-dimensional operator for bank failures induced by water-level rise in dam-break flows. *Journal of Hydraulic Research* **48** (3), 302–314.

Tropea, C., Yarin, A. & Foss, J. 2007 *Handbook of Experimental Fluid Mechanics*. Springer-Verlag. Q7

Van Emelen, S., Zech, Y. & Soares-Frazão, S. 2015 Impact of sediment transport formulations on breaching modelling. *Journal of Hydraulic Research* **53** (1), 60–72.

Vano, J. A., Dettinger, M. D., Cifelli, R., Curtis, D., Dufour, A., Miller, K., Olsen, J. R. & Wilson, A. M. 2019 Hydroclimatic extremes as challenges for the water management community: lessons from Oroville dam and hurricane Harvey. *Bulletin of the American Meteorological Society* **100** (1), S9–S14.

Visser, P. J. 1995 *Application of sediment transport formulae to sand-dike breach erosion*. Communications on Hydraulic & Geotechnical Engineering, 94(7), 78 p. Delft University of Technology, Delft, The Netherlands.

Zou, X., Wang, C., Song, H., Han, Z., Ma, Z. & Hu, W. 2018 Applications of ultrasound imaging system for measuring water-sand parameters during sediment transport process in hydraulic model experiments. *Journal of Hydroinformatics* **20** (2), 410–423.

First received 31 January 2020; accepted in revised form 22 May 2020. Available online 29 June 2020

Author Queries

Journal: Journal of Hydroinformatics

Manuscript: HYDRO-D-20-00026

Q1 Please indicate which authors, if any, are IWA members.

Q2 Koksinas *et al*. (2019) has been changed to Koskinas *et al*. (2019) as per the reference list. Please check.

Q3 Please provide the expansion of the acronym [DTM].

Q4 Swartenbroecks *et al*. (2010) has been changed to Swartenbroekx *et al*. (2010) as per the reference list. Please check.

Q5 Please provide the conference date and location for the reference 'Frank and Hager (2014)'.

Q6 Please provide missing city for the reference 'Raffel *et al.* 2007'.

Q7 Please provide missing city for the reference 'Tropea *et al.* 2007'.

Q8 In supplied Figure 7 is not sufficient print quality. Please resupply as a high resolution file (300 dpi or above) with sharp lines and text.

Q9 In supplied Figure 9 is not sufficient print quality. Please resupply as a high resolution file (300 dpi or above) with sharp lines and text.

Q10 In supplied Figure 11 is not sufficient print quality. Please resupply as a high resolution file (300 dpi or above) with sharp lines and text.

Q11 In supplied Figure 13 is not sufficient print quality. Please resupply as a high resolution file (300 dpi or above) with sharp lines and text.

Q12 In supplied Figure 17 is not sufficient print quality. Please resupply as a high resolution file (300 dpi or above) with sharp lines and text.

Q13 In supplied Figure 18 is not sufficient print quality. Please resupply as a high resolution file (300 dpi or above) with sharp lines and text.